Journal of Power Sources 253 (2014) 90–97

Contents lists available at ScienceDirect

Journal of Power Sources

journal homepage: www.elsevier.com/locate/jpowsour

Post-mortem analysis of a long-term tested proton exchange membrane fuel cell stack under low cathode humidification conditions

Nam-In Kim [a], Yongho Seo [a], Ki Buem Kim [a], Naesung Lee [a], Jin-Hwa Lee [b], Inseob Song [b], Hanshin Choi [c], Jun-Young Park [a,*]

[a] HMC & INAME, Green Energy Research Institute, Faculty of Nanotechnology and Advanced Materials Engineering, Sejong University, 98 Gunja-dong, Gwangjin-gu, Seoul 143-747, Republic of Korea
[b] Fuel Cell Group, Energy Lab, Samsung SDI Co., LTD, 575 Shin-dong, Yeongtong-gu, Suwon-si, Gyeonggi-do 443-391, Republic of Korea
[c] Rare Metals Research Group, Korea Institute of Industrial Technology, Incheon 404-254, Republic of Korea

HIGHLIGHTS

- Durability tests for PEMFC stacks are carried out in constant power mode with simulated reformate fuel gases.
- Major degradation mechanisms and patterns in a PEMFC stack are investigated under low cathode humidification.
- Various post-mortem investigations are carried out to disclose the main reasons of failure of the stack.
- Delamination of the catalyst layer of unstable operating MEAs is significant near the cathode gas inlets.
- Degradation is due to the cathode carbon corrosion and membrane failure during the start-up and shut-down process.

ARTICLE INFO

Article history:
Received 4 September 2013
Received in revised form
13 November 2013
Accepted 13 November 2013
Available online 1 December 2013

Keywords:
Proton exchange membrane fuel cell
Stack
Durability
Degradation
Low humidity conditions
Post-mortem analysis

ABSTRACT

During continuous power operation for 2740 h, the major mechanisms and patterns of performance degradation in a polymer electrolyte membrane fuel cell (PEMFC) stack are investigated under low cathode humidification with simulated reformate fuel gases through the use of various physicochemical and electrochemical analysis tools. As operating time increases, the operating voltages and open-circuit voltages (OCVs) of the stack decrease with the large voltage distributions. In the post-mortem analysis of the stack, the delamination of the catalyst layer (CL) of unstable operating membrane electrode assemblies (MEAs) is significant near the cathode gas inlets. This observation is in agreement with the results of OCV, hydrogen crossover current, and anode off-gas measurements. This phenomenon may be due to the acceleration of carbon corrosion in the cathode during the frequent start-up and shut-down process, because the local cathode potential can reach more than 1.5 V in the air/fuel boundary. Additionally, the frequent membrane hydration and dehydration by the accumulation of excess water (through electrochemical reaction) and faster water evaporation (under dry-air cathode conditions and high operating temperatures) may accelerate the interface delamination between the membrane and cathode CL with a substantially uneven distribution of water.

1. Introduction

One of the remaining technical challenges for the commercialization of polymer electrolyte membrane fuel cells (PEMFCs) for portable, stationary, and transport applications is to assure long-term durability and high reliability with reduced system cost [1,2]. The lifetime targets for 2015 set by the U.S. Department of Energy (DOE) is at least 5000 h for automobile applications and 40,000 h for building applications under practical operating conditions. The costs of manufacturing PEMFC systems (including materials) must also be reduced concurrently [3]. Over the last decade, much research has been conducted to improve the long-term durability of PEMFCs by improving membranes, anode/cathode catalysts, bipolar plate materials, balance-of-plants (BOPs), and operating logics (start-up–shut-down) [4–6]. Among these, one of the major cost components in manufacturing PEMFCs for various

* Corresponding author. Tel.: +82 2 3408 3848; fax: +82 2 3408 4342.
E-mail address: jyoung@sejong.ac.kr (J.-Y. Park).

0378-7753/$ – see front matter © 2013 Elsevier B.V. All rights reserved.
http://dx.doi.org/10.1016/j.jpowsour.2013.11.056

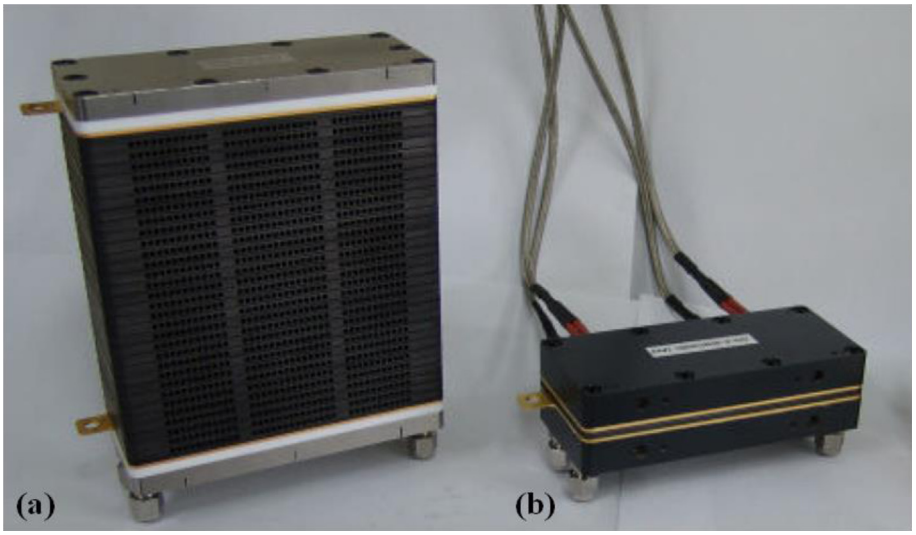

Fig. 1. Exterior view of the (a) 32-cell and (b) single-cell PEMFC stack. The closest cell from the gas inlet (bottom) was designated as #1 (bottom) and the far-end cell (up) from the gas inlet was designated as #32.

applications is the catalyst and bipolar plate. Extensive works have carried out to reduce the cost via the use of more effective supports (*e.g.* graphene, nanofibers, and nanoparticles) and novel composite catalysts (Pt alloys with various transition metals) with less precious metal loadings, and high-performance membrane electrode assemblies (MEAs) with better fabrication methods and electrode structure [7,8]. Low-cost bipolar materials such as composite materials or other conductive metals have also been considered as alternatives to graphite plates, in terms of the conductivity, gas permeability, corrosion resistance, ease of manufacturability, thinness, and light weight [9].

Another way to realize cost-savings for PEMFC systems is to remove the external gas humidification parts on the cathode side [10]. It is possible to minimize the complexity, size, and number of balance-of-plants (BOPs) in PEMFC systems. The high humidification of gas causes additional energy losses due to the heating of the humidifier and control of the water balance [11]. Additionally, at subzero temperatures, detrimental effects by ice formation on PEFMCs (*e.g.* in the MEAs and humidification parts) in the cathode part can be reduced during the storage and operation of the system. Low-humidified fuels, however, may reduce the lifetime of PEMFCs with reduced power density due to the dehydration and mechanical stress of the membrane by uneven water distribution between both the electrodes in the MEA.

Hence, this study aims at assessing the major mechanisms and patterns of performance degradation in a PEMFC stack (including membranes, electrodes, bipolar plates, and seals) operating continuously for thousands of hours under low cathode humidification through the use of various physicochemical and electrochemical analysis tools. Although many efforts have been made on understanding PEMFC behavior under low-humidification conditions, they have mainly focused on stable stack performance without humidifying the gas streams through the specific design of a stack flow-field or proper operating conditions [11–13]. In addition, it is imperative that the long-term durability of PEMFC stack be evaluated as a function of time under realistic operating conditions to enter the energy market, since single-cell evaluation cannot represent the characteristics of a PEMFC system in terms of energy and thermal efficiency due to the non-uniformity in potential, temperature, and flow distributions [14].

The CO tolerance of a PEMFC stack is also investigated with liquefied petroleum gas (LPG) reformed hydrogen gas containing a few ppm of CO in the anode for various power applications. At present, LPG is easily accessible and available without major infrastructure investment. Most previous research has mainly been conducted in mild operating conditions using hydrogen fuel, full humidification, and constant operation mode regarding voltage or current. This work contributes to recognizing various degradation sources occurring under harsh PEMFC operation conditions to realize stable stack performance in a real operation mode for a targeted lifetime.

2. Experimental

2.1. Stack preparations

Membrane electrode assemblies (MEAs) were prepared by a commercial catalyst-coated membrane (CCM; Gore MESGA Primea Series, USA) with Pt–Ru/C (anode) and Pt/C (cathode) catalysts. The Pt loadings were 0.4 $mgcm^{-2}$ for both electrodes, and SGL carbon papers (35BC Germany) were used as gas diffusion layers (GDLs). The active area of the electrode was 51.6 cm^2 for MEAs in the stack. The PEMFC stack was composed of 32 single cells connected in series with machined-graphite flow-distribution plates (Ildo F & C, Korea). A planar PEMFC stack is shown in Fig. 1, where the closest cell from the gas inlet is designated as #1 (the lowest cell), and the cell at the far end from the gas inlet was designated as #32 (the highest cell). The flow channels of the cathode and anode were designed as quadruple and dual serpentine-type fields, respectively, and their width and depth were 0.3 mm and 1.0 mm, respectively. Ethylene propylene diene monomer (EPDM; Don-A Hwa Sung Co, Korea) was used for the gasket between each single cell for its chemical resistibility and stability. The six cooling fans (GB0535AEV2-8, Sunon, Taiwan) were set up on the front of the stack for quick removal of the heat generated by high-temperature humidified fuel and electrochemical reactions inside the stack. Cell voltage probes were installed on the side of the stack to read the voltage variation of 32 cells.

2.2. Stack durability test

A durability test was carried out with the PEMFC stack using a fuel cell test station (Arbin Instruments, USA) equipped with an electrical load, mass flow controllers (MFCs), temperature-variable

humidifiers, and gas line heaters. The operating characteristics of the PEMFC stack were investigated in constant power modes (300 W → 280 W → 260 W) with real simulated operating conditions for 10 h on and 2 h off. The stack temperature was regulated at 65 °C by external cooling fans, and three thermocouples were placed at the centers of cells (#1, #16, and #32) to monitor the temperature distribution inside the stack. The stack was fed with humidified simulated-fuel processed gases (H_2 70%, N_2 6.5%, CH_4 0.998%, CO_2 22.5%, CO 20 ppm) and dry air with stoichiometries of 1.75 and 2.80, respectively, at ambient pressure. The humidification for the anode fuel was controlled by changing the humidifier bottle temperature (58 °C). Air-bleeding method (200 ml min^{-1} air) [15] was used to control the CO contained in the reformed gas, because trace levels of CO can substantially decrease the stack performance. The safety logic comprised an automatic shut-down at under 0.45 V of voltage for each cell to prevent failure of the PEMFC stack.

2.3. Post-mortem analysis of PEMFC stack

After the durability experiment, the degradation mechanisms of the PEMFC stack were investigated by various physicochemical and electrochemical analysis tools. First, the influences of changes in stoichiometry on the current–voltage performance recovery were examined by increasing the anode fuel stoichiometry from 1.75 to 2.00 and the cathode stoichiometry from 2.80 to 3.80 under a constant power of 240 W to examine the mass transport limitations of the stack. In order to evaluate the hydrogen crossover and electronic shorting in the MEAs, constituent analysis of the anode off-gas (AOG) and linear sweep voltammetry (LSV) were performed before and after the durability test. The AOG components were analyzed by gas analyzer (Horiba, Japan) in the OCV state. Humidified fuel processed gases and dry air were fed into the PEMFC stack at 65 °C. LSV measurements were obtained for the H_2/N_2 cell with a potential range of 1.0–5.0 V using an electrochemical analyzer (Solartron Analytical 1470E, UK).

After the durability test, stack MEAs with unstable performance were reassembled into a single short-stack with gaskets, bipolar plates, and GDLs (fresh and tested) for further electrochemical investigations, as shown in Fig. 1b. Electrochemical impedance spectroscopy (EIS) was carried out to analyze the ionic resistances of the membrane and catalyst layer (CL), as well as the charge transfer resistance and the mass transfer resistance. EIS measurements were conducted in the frequency range of 10 kHz–100 mHz using a potentiostat (Solartron Analytical 1287, UK) in conjunction with a frequency response analyzer (Solartron Analytical 1255B, UK), and a power booster (Solartron Analytical, 1290, UK). The amplitude of the sinusoidal voltage signal was within 10 mV. The contact angles of GDL (SGL 35BC, Germany) surface before and after the on/off durability cycles were measured by the sessile-drop test using a contact angle system (DSA 100, Krvss, Germany). The contact angle was measured at 15 s after a droplet of water (15 μl pure water droplet) touched the solid surface. The heights of gaskets and clearances between the cells in PEMFC stack were measured by the profile projector (gasket measurement system, VMS, Korea) after the durability test.

3. Results and discussion

3.1. Stack durability test

The cell voltage and current density of the PEMFC stack are shown in Fig. 2 for the entire 2740 h life test as a function of time under constant power mode (300 W → 280 W → 260 W). Simulated reformate gases and dry air were used at ambient pressure as the anode and cathode reactants, respectively. The initial performance of the stack operated under a constant power of 300 W with highly humidified fuels maintained at 65 °C was 0.729 V on average (Fig. 2a). The required voltage was decreased from 0.729 to 0.658 V to maintain the specified power output over time, while the current showed an upward tendency from the initial value of around 0.260 Acm^{-2}. The difference in performance between the difference operating voltage and increasing current gradually increased with time in the durability test. Unfortunately, the PEMFC stack could not be stably operated at 300 W after testing for 2060 h. Several cells (#5, #20, and #22) showed a voltage lower than 0.64 V during continuous operation after 1890 h, and voltage drops suddenly occurred below 0.1 V, resulting in the unintentional shut-down of the stack by the automated safety operation logic. Hence, the PEMFC stack was then operated at 280 W for 2450 h and 260 W 2740 h for the same reason.

The operating stability of the stack was evaluated by cell-to-cell voltage variations in continuous power operation mode. The voltage distributions across the entire 32-cell stack were monitored at 65 °C, and the results are shown in Fig. 2b. All standard deviations of the voltages were calculated as the average values after steady-state conditions for 1 h over a period of 10 h. The cell voltage distribution became increasingly less uniform with the aging process. This increased significantly from 5.0 to 35.8 mV, and the voltage difference between the maximum and minimum also increased from 30 to 153 mV. The voltage distributions of cells in the PEMFC stack during 10 h of operation before and after durability testing are shown in Fig. 3. For the initial state (Fig. 3a), the

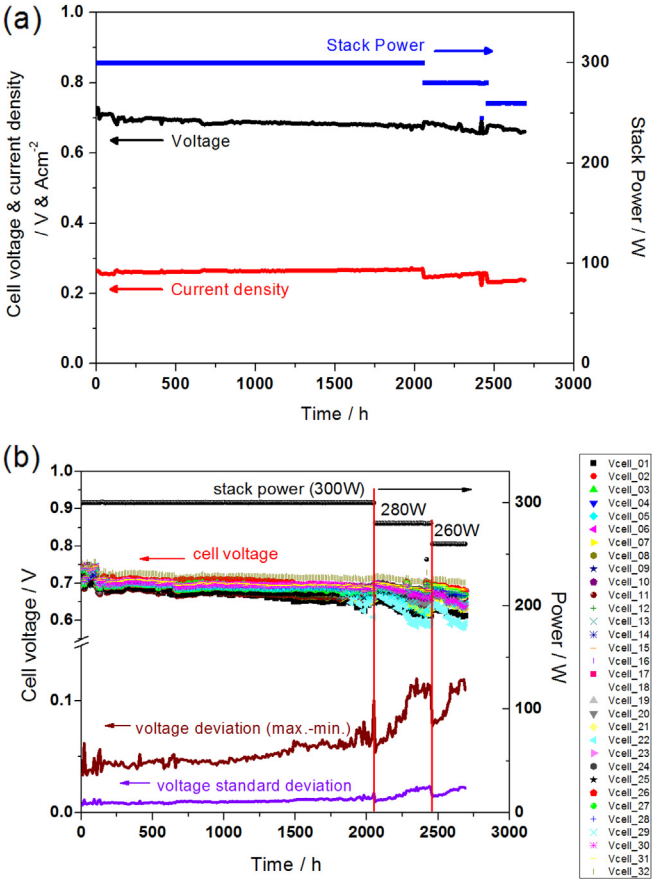

Fig. 2. (a) Cell performance by voltage and current density, and (b) the operating stability of PEMFC stack by cell-to-cell voltage variations for the entire 2740-h life test as a function of time under the constant power mode (300 W → 280 W → 260 W).

voltage variations of the stack at a constant power of 300 W are highly uniform within 5 mV. As the operating time increased, however, the operating voltage decreased with large voltage distributions (Fig. 3b). The voltages of individual cells in the operating state are shown in Fig. 3c to fully recognize inferior cells in the PEMFC. The average voltage of a stack under constant-power operation is 0.729 V with small distributions in the initial state, whereas several cells (#6, 7, 20, 22, and 30) showed unstable performance with decreased cell voltage after the durability test. In order to understand this phenomenon, the dominant degradation mechanisms are analyzed in the next section.

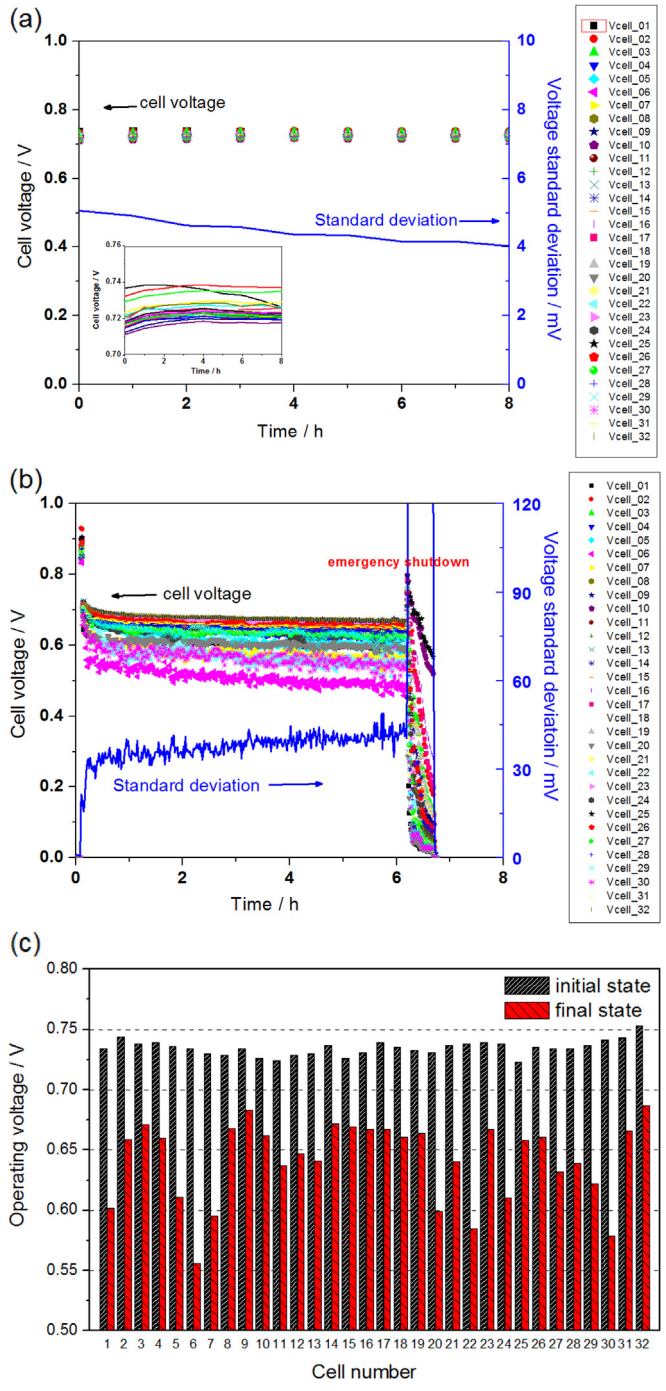

Fig. 3. Voltage distributions of cells on PEMFC stack during 10 h of operation (a) before and (b) after durability testing, and (c) voltages of individual cells under operating state to recognize inferior cells in stack.

3.2. Analysis of pre-disassembly of stack

PEMFC stack degradation has been reported in several studies [16–21]. The main degradation mechanism is related to the reduction in the electrochemical active surface area by the sintering and agglomeration of Pt, carbon oxidation, membrane thinning, reduced interfacial strength between the electrodes and membranes, corrosion of the stainless steel BPs, and poisoning of the MEAs by metal dissolution [22–24]. However, additional studies are necessary to determine the PEMFC degradation behavior under low-humidification conditions with the simulated reformate fuel. Post-mortem analysis of the PEMFC stack was carried out to determine the main cause of degradation. After durability testing for 1800 h under 300 W constant-power operation, the non-uniformity of the PEMFC stack regarding cell voltages was observed. In particular, cells #5, #20, and #22 showed substantial voltage fluctuations during 6 h of operation, as shown in Fig. 4. This phenomenon is generally attributed to the mass transport limitation by the high rates of water production, which led to flooding.

For clear understanding of the effect of the mass transport limitation in both electrodes, the anode and cathode fuel stoichiometry was changed, and the cell voltage standard deviations and $[V_{max}-V_{min}]$ values were measured. As shown in Fig. 5, the cell voltage standard deviations and $[V_{max}-V_{min}]$ values increased drastically from 5.0 and 30.0 mV in the initial state to 35.8 and 153.1 mV, respectively, in the final state (Fig. 5a and b). In order to decrease the mass transport limitation on the cathode side, the air stoichiometry was increased from 2.8 to 3.8. Increasing the cathode air stoichiometry, however, resulted in a negligible change in the cell voltage standard deviation and $[V_{max}-V_{min}]$ values (Fig. 5c). This means that cathode water flooding can be eradicated as a main cause of unstable stack performance under dry-air cathode operation. In contrast, increasing the anode fuel stoichiometry from 1.75 to 2.00 resulted in decreasing the cell voltage standard deviations and $[V_{max}-V_{min}]$ to values of 24.3 mV and 108.3 mV, respectively (Fig. 5d). This means that anode mass transport limitations contributed to the voltage degradation of the stack to some extent, since the anode was operated continuously with humidified reformate gases. Though the cell voltage stability and uniformity showed slight improvements under constant-power operation, the PEMFC stack still could not be stably operated at 300 W with an increased fuel flow rate. This means that other principal degradation mechanisms should be considered, even though the mass transport limitation on the anode side had some effect on the stack performance.

It has been shown that the performance decay rate of an MEA is dependent on the membrane degradation, such as thinning, hole formation, and contamination (silicon, metal cations) in the MEA components [25–27]. A common diagnostic tool in stack testing is the measurement of individual cell voltages at open-circuit voltage (OCV). These measured variations can be used as a means to recognize degraded membranes in MEAs. OCVs of 32 cells in a PEMFC stack were measured before and after the durability testing, and the results are shown in Fig. 6. In the initial state of the long-term test, the OCV of the stack was 31.2 V, with the average OCV of each unit cell being 0.976 V. After durability testing, the cell voltages showed a large discrepancy throughout the stack. The OCVs of the 32 cells varied from 0.80 V to 0.93 V after 2740 h of testing. In particular, 6 cells (#5, 6, 7, 20, 22, and 30) showed a lower voltage of 0.8 V. The low OCV was inferred to have come from membrane failure or MEA delamination. This voltage non-uniformity and low OCV may be due to the increased hydrogen crossover through the polymer electrolyte membrane, resulting in the mixed potential in the cathode. These phenomena are strongly correlated to mechanical and chemical failures by creep of the

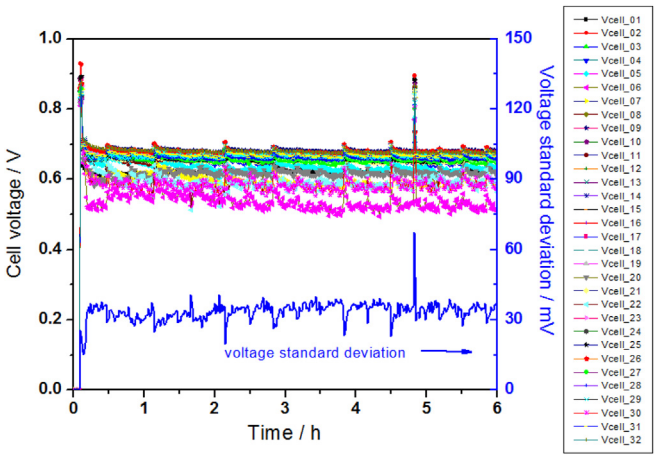

Fig. 4. Non-uniformity in cell voltages of PEMFC stack with the substantial voltage fluctuations during 6 h operation.

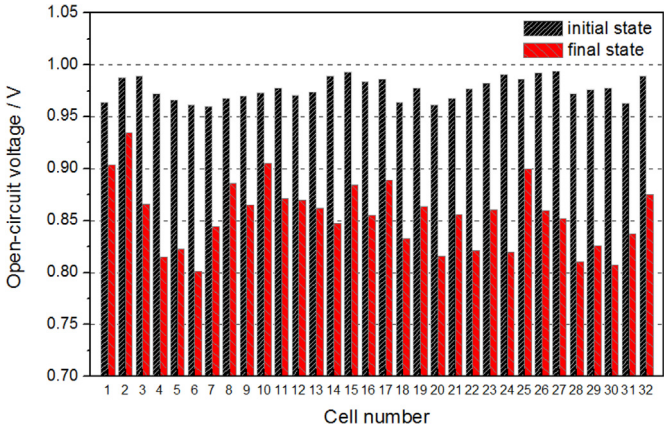

Fig. 6. OCVs of 32 cells in PEMFC stack measured before and after the durability testing.

polymer electrolyte membrane [28–30]. The polymeric membrane is exposed to frequent swelling and contraction conditions due to the accumulation of excess water and shortages due to faster water evaporation at high operating temperatures by frequent start-up and shut-down cycles. A sizable volume change of the polymeric membrane at a high operating temperature can amplify the mechanical stress at the interface. The mechanical and chemical failure modes of the membrane are strongly correlated to the PEMFC operation.

In order to confirm this explanation, the compositions of the anode off-gas (AOG) were measured by a gas analyzer, and the results are shown in Table 1. The amount of hydrogen in the AOG showed a big difference of 17.3% between before and after the durability testing of the stack. This large difference is ascribed to the increased hydrogen crossover by severe membrane thinning or pin-holes. Hydrogen crossover through the membrane leads to decreased efficiency of the fuels. This result was also confirmed by measurement of the hydrogen crossover current of the proton exchange membrane via linear sweep voltammetry (LSV) [31,32]. LSV curves of the fresh MEA and after 2740 h are shown in Fig. 7. Hydrogen crossover is evaluated by the diffusion-limited hydrogen oxidation current obtained at 3 V. By dividing the current by the active area, the hydrogen current density of the stack drastically increased from 0.58 mAcm^{-2} to 30.4 mAcm^{-2} (fifty times greater) during the constant-power operation. This result indicates that membranes in the stack deteriorated considerably, which could also be confirmed from the variation in the OCV and AOG analysis. The performance degradation in the PEMFC stack was thus mainly caused by the decay of the proton exchange membrane under low cathode humidification conditions.

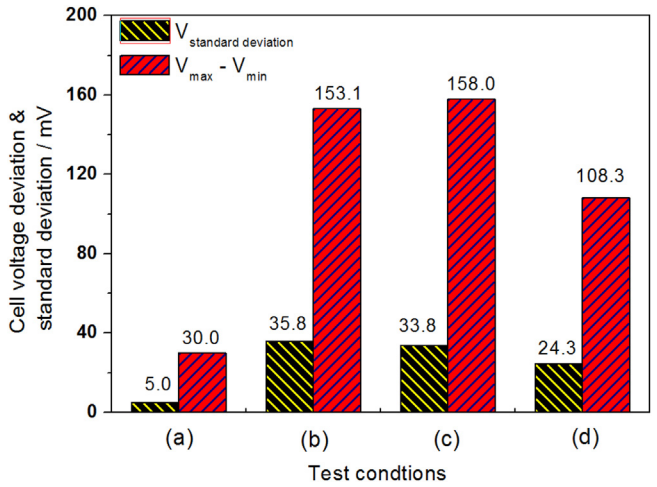

Fig. 5. Comparisons of cell voltage standard deviations and [V_{max}–V_{min}] values: (a) in the initial state; (b) in the final state; (c) in the increasing of cathode air stoichiometry from 2.8 to 3.8; and (d) in the increasing of anode fuel stoichiometry from 1.75 to 2.00.

3.3. Analysis of post-disassembly of stack

At the end of the 2740 h durability test, the PEMFC stack was carefully disassembled for further investigations. In order to probe the degradation mechanism of the unstable stack MEAs under constant-power operations in detail, the MEAs of the 20th and 22nd cells from the bottom of the stack were taken out. Both CCMs were reassembled into single short-stacks (Fig. 1b) with original degraded GDLs and fresh GDLs. The performance of the single short-stacks was measured under 80% relative humidity (RH) H_2 (stoichiometry of 1.5) and dry air (stoichiometry of 2.5), at 100 mAcm^{-2} and 65 °C. As shown in Fig. 8, the voltage of the 20th and 22nd cells decreased from 0.8 V to 0.705 V and 0.725 V, respectively, after the durability test. Even with fresh GDLs, the cell performance was still lower compared to that of the initial state of the stacked MEAs, even though the MEA performance was partially recovered.

To provide further evidence of the reasonable interference, electrochemical impedance spectroscopy (EIS) analysis was performed for each single short-stack under galvanostatic control at 100 mAcm^{-2} and 65 °C. Measurements were taken at the 20th and 22nd cells before and after replacing the GDLs with a fresh stack of MEAs to acquire reference values of the resistances. In the Nyquist plots of the single short-stacks in Fig. 9, (i) the real intercept with the real axis at high frequency represents the ohmic resistance

Table 1
Compositions of anode off-gas (AOG) measured by gas analyzer before and after the durability testing.

Gas/unit	Anode in-gas concentrations	Anode off-gas initial state	Anode off-gas after durability testing
H_2/%	70	51.5	34.2
CO/ppm	20	3.4	1.6
CO_2/%	22.5	35.6	41.3
CH_4/%	0.998	2.0	2.1

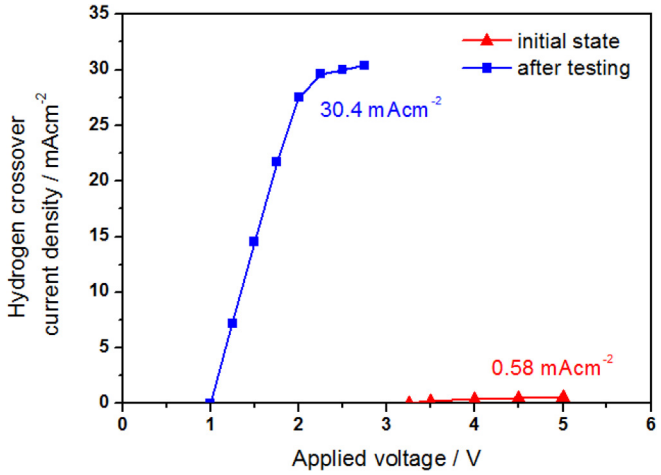

Fig. 7. Measurements of the hydrogen crossover current of the PEMFC stack via linear sweep voltammetry of the fresh MEA and after 2740 h.

(R_{ohmic}) of the cell, which includes the polymer electrolyte membrane; (ii) the linear region starting from the intercept on the Z' axis represents the contribution from the ionic conduction (R_{cl}) through the catalyst layer; and the (iii) mid-frequency and (iv) low-frequency intercepts correspond to the charge transfer (R_{ct}) and mass transfer resistance (R_{mt}) of the cell, respectively [33–36].

The results of the fitting of the equivalent circuit model to the semicircles are presented in Fig. 10. The R_{ohmic} during 2740 cycles increased from 0.448 to 0.505 (cell #20) and 0.485 Ωcm^2 (cell #22) for 80% RH H_2 and dry air cells. Among the resistance components of the MEA, R_{ct} and R_{mt} increased significantly after the durability testing. In addition, the impedance spectra show unsteady noise patterns at a low-frequency range of the complex plane plot after the electrochemical stresses with constant power, as shown in Fig. 9. This finding indicates that the increase in resistance by cathode deterioration is one of the dominant factors in the degradation mechanisms, because the lower-frequency arc is related to the mass transport process [36]. Furthermore, the contribution from the anode can be ignored, because of the much faster hydrogen oxidation reaction than the oxygen reduction. To see the effect of mass transport limitation on the degraded MEA performance, the original degraded GDLs of single short-stacks were

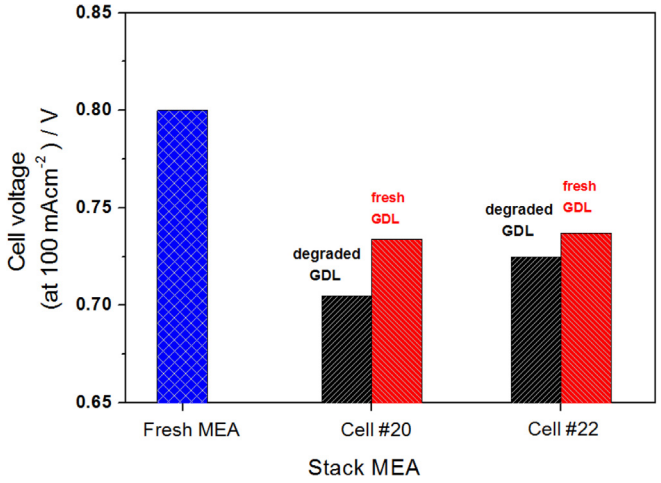

Fig. 8. Performances of the single short-stacks (20th and 22nd cells) with original degraded and fresh GDLs measured under 80% RH of H_2, dry air, 100 mA cm^{-2}, and 65 °C.

replaced with fresh GDLs, and EIS measurements were then carried out in the same conditions as shown in Fig. 10. Interestingly, the R_{ohmic} increased from 0.505 to 0.550 Ωcm^2 (cell #20) and from 0.485 to 0.537 Ωcm^2 (cell #22) for 80% RH H_2 and dry air cells. On the other hand, the change of GDLs for cell #20 and cell #22 resulted in significantly decreasing R_{mt} from 0.752 and 0.498 Ωcm^2 to 0.154 and 0.21 Ωcm^2 in cell #20 and cell #22, respectively. The increased R_{ohmic} of degraded MEAs by fresh GDLs might be due to poor interface (mechanical integrity) between the CCM and new GDLs, since degraded CCMs were tested more than 2740 h. Since the loss of the PTFE should accompany the change in mass transport properties of the diffusion layer, water contact angle can be a measure of the degradation of GDLs. The contact angles of GDLs (SGL 35BC) were measured to analyze the water management properties of MEAs. PTFE on GDLs provides high hydrophobicity (with high contact angle) to avoid water flooding. The contact angles of GDL decreased from 149.3° (pristine state) to 139.2° (anode inlet), 130.4° (anode outlet), 134.8° (cathode inlet), and 129.3° (cathode outlet), after the durability test. The results for water contact angle means that the mechanical degradation of cathode GDL happens during the durability test. The reduction of the mass transfer resistance alone, however, could not entirely explain the performance degradation factor of MEAs, which was in agreement with the experimental results of the gas flow rate change, as mentioned in the previous section.

Further, in order to investigate the decay mechanism of the unstable MEAs, the compression uniformity of a PEMFC stack was evaluated by sectional heights of gaskets for both electrodes and clearances between the cells. Before the durability test, the compression ratio of the MEA was adjusted with compressible gaskets (EPDM), which varied in thickness. Bolts through the two end plates were fastened down using a torque wrench so that even pressure was applied throughout the entire surface of the end plates. Post-test visual examinations of the stack showed that significant degradation of the anode and cathode gaskets was not occurred in the cells. Fig. 11 shows the measured heights of gaskets and clearances between the cells after the durability test. The significant change of the EPDM gaskets in sectional heights and clearances in cathode inlet and outlet was not occurred in the stack and there is no relationship between gasket heights and clearance and performance in degraded MEAs.

After the single short-stack test, several cells (#10, #16, and #30) were carefully disassembled for further analysis. Cell #30 showed unstable performance with reduced operating voltage (highly degraded CCM), whereas the performance degradation of cells #10 and #16 was relatively low (slightly degraded CCM). Fig. 12 shows the optical image of the cathode side of CCMs. It was observed in cell #30 that the dissolution of the cathode catalyst layer and interface delamination between the CL and membrane was significant, as shown in Fig. 11a. Slightly degraded CCMs (#10 and #16) showed some pin-holes and CL loss on the cathode side (Fig. 11b). The delamination of the CL was particularly severe near the cathode gas inlets, which were reaction sites for dry air with transported protons through the membrane. Likewise, identical CL degradation was found in unstably operating MEAs (#5, #6, #7, #20, and #22) in the post-mortem analysis stack. This observation was in agreement with the results of the OCV, hydrogen crossover current measurements, and AOG analysis. In addition, the loss of the cathode CL at the gas inlet region may be due to the frequent start-up and shut-down process of the cells. It was demonstrated that the start-up and shut-down resulted in a kind of carbon corrosion in the form of cracking or delamination of the CL, as well as catalyst ripening and ionomer dissolution [37–39]. This is because the local cathode potential can reach more than 1.5 V in the air/fuel boundary due to partial hydrogen coverage in the anodes,

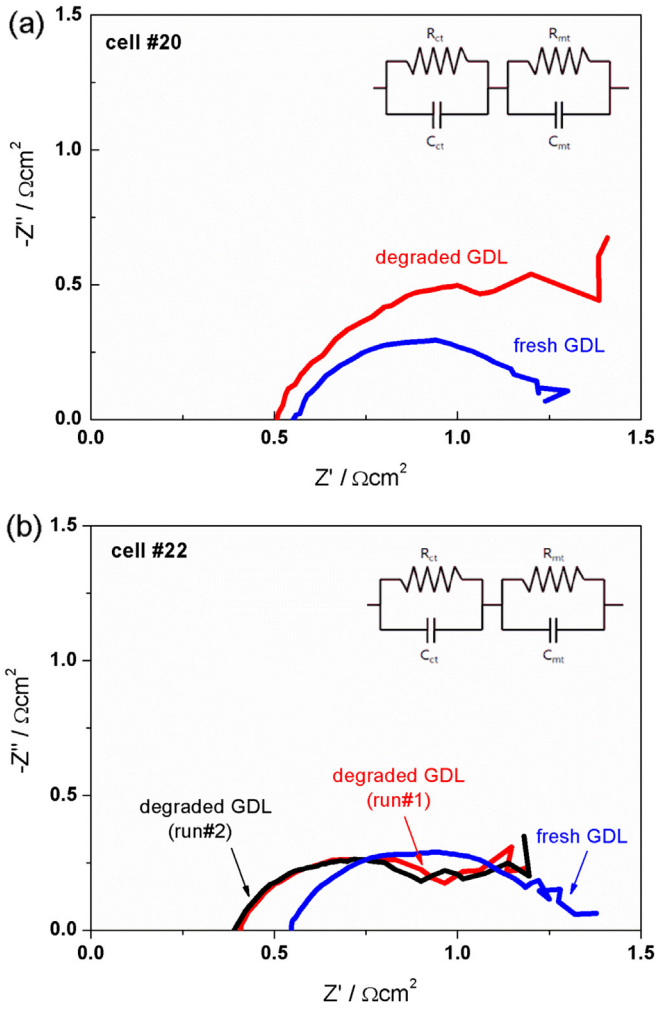

Fig. 9. EIS analysis of each single short-stack [(a) 20th and (b) 22nd cells] with original degraded and fresh GDLs performed under galvanostatic control at 100 mAcm^{-2} and 65 °C.

which drastically accelerates carbon corrosion in the cathode. In addition, carbon corrosion also arises from the crossover of reactant gas through the membrane. Furthermore, interface degradation occurred on the cathode side of the MEA through mechanical and chemical failure modes by polymeric membrane swelling and contraction, which is strongly correlated to the PEMFC operation. This phenomenon can be attributed mainly to the recurrent membrane hydration and dehydration by the accumulation of excess water (through electrochemical reaction) and faster water evaporation, under high operating temperatures and dry-air cathode conditions [28–30]. An extensive volume change can amplify the mechanical and chemical stress at the interface. Additionally, the uneven distribution of water between the anode and cathode through the membrane may bring about incessant stress on the interface during long-term PEMFC stack operation, because the anode side is continuously experiencing humidified conditions, whereas the cathode is alternatively exposed to dry and wet states. The chemical degradation of the membrane can also proceed via peroxide radical attack during the durability test [40–42]. It is commonly believed that decomposition of the membrane is caused by the chemical attack of hydroxyl and hydroperoxyl radicals generated by the reaction between H_2 and O_2. This attack makes the membrane degrade, resulting in the increase of hydrogen permeation.

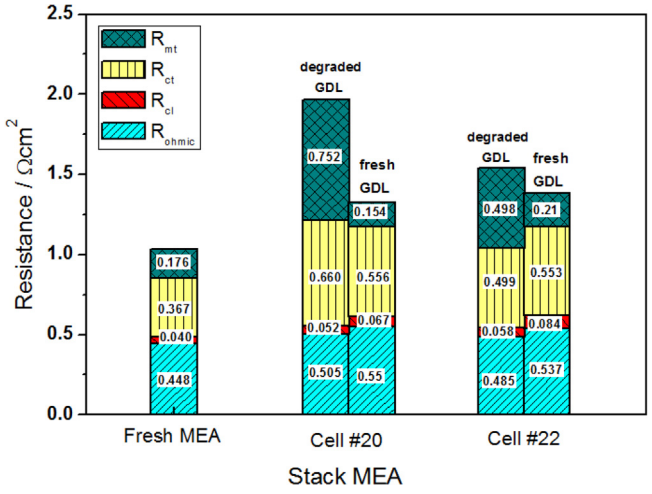

Fig. 10. Analysis results of the fitting of the equivalent circuit model to the semicircles of each single short-stack [(a) 20th and (b) 22nd cells] with original degraded and fresh GDLs.

4. Conclusions

Durability tests for PEMFC stacks were carried out in constant power mode under low cathode humidification with simulated

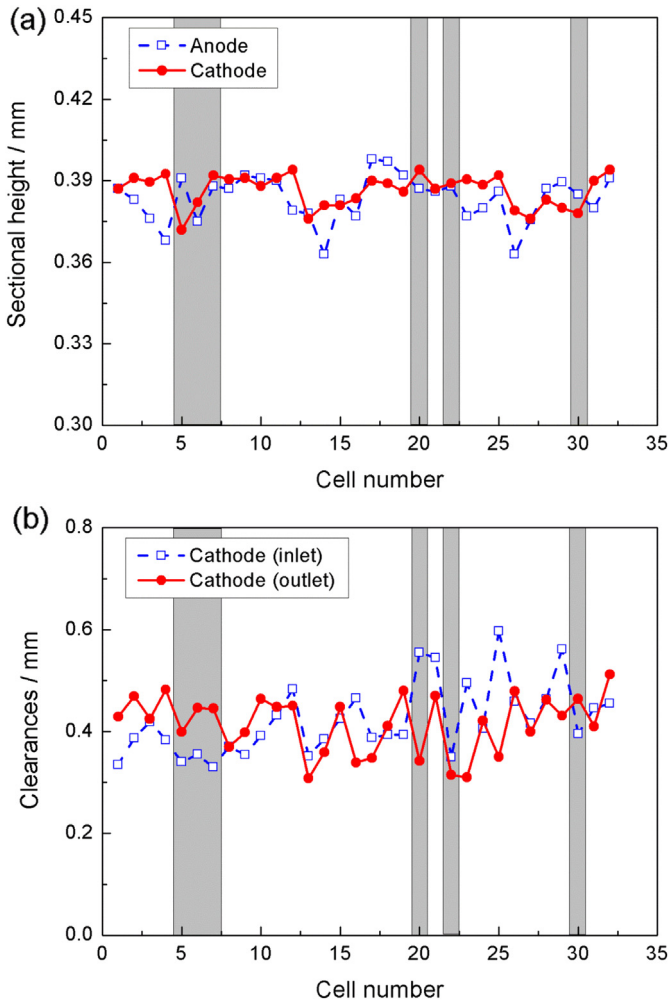

Fig. 11. Measured (a) sectional heights of gaskets and (b) clearances between the cells after the durability test. Each block represents unstable performance MEAs.

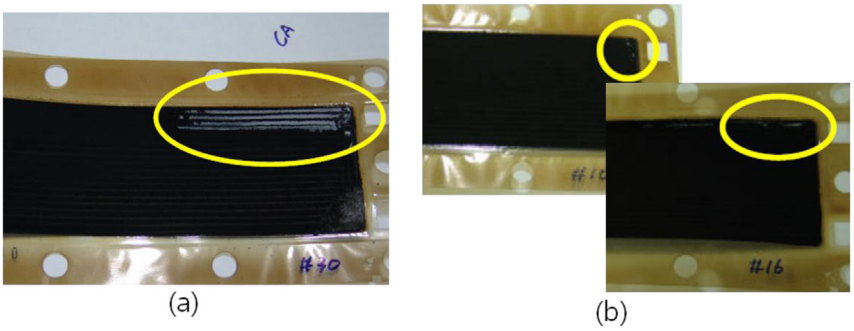

Fig. 12. Optical image of cathode side of CCMs after 2740 h testing: (a) highly degraded CCM (#30); (b) slightly degraded CCM (#10 and #16).

reformate fuel gases. During the entire durability testing time, the performance of the stack decreased steadily, and the stack abruptly could not be operated stably under constant power mode after 2740 h of testing, due to the output of several unstable cells decreasing to below 0 V. Various post-mortem investigations were carried out to disclose the main reasons of failure of the stack, such as the change of the anode and cathode fuel stoichiometry, OCV, hydrogen crossover current, AOG, and EIS analysis. In the results of pre-disassembly and post-disassembly analysis, it was found that the mass transport limitation and anode flooding by degraded GDLs had an important effect on decreasing the cell performance of the PEMFC stack during long-term durability tests. Most importantly, the delamination of CLs of unstably operating MEAs in the stack was particularly severe near the cathode gas inlets. This phenomenon might be due to the frequent start-up and shut-down process of the cells, which resulted in accelerating the carbon corrosion by high local cathode potential in the air/fuel boundary. This was also strongly correlated to the mechanical and chemical failure modes by polymeric membrane swelling and contraction under high operating temperatures and particularly dry-air cathode conditions, and could amplify the mechanical and chemical stress at the interface with the uneven distribution of water between the anode and cathode through the membrane. Chemical degradation of the membrane could also proceed via peroxide radical attack generated by the reaction between H_2 and O_2 during the durability test.

Acknowledgments

This study was supported by the New & Renewable Energy project of a Korea Institute of Energy Technology Evaluation and Planning (KETEP) grant funded by the Korean Ministry of Knowledge Economy (No. 2011T100200280), the Fundamental R&D Program for Core Technology of Materials funded by the Ministry of Knowledge Economy (#10037289, Development of Highly Active and Sustainable Hybrid Catalysts), and the Fusion Research Program for Green Technologies through the National Research Foundation of Korea (NRF, #2011-0004428).

References

[1] M.C. Williams, J.P. Strakey, W.A. Surdoval, J. Power Sources 143 (2005) 191–196.
[2] M.W. Fowler, R.F. Mann, J.C. Amphlett, B.A. Peppley, P.R. Roberge, J. Power Sources 106 (2002) 274–283.
[3] S.D. Knights, K.M. Colbow, J. St-Pierre, D.P. Wilkinson, J. Power Sources 127 (2004) 127–134.
[4] A. Taniguchi, B.T. Akita, B.K. Yasuda, Y. Miyazaki, J. Power Sources 130 (2004) 42–49.
[5] D.E. Curtin, R.D. Lousenberg, T.J. Henry, P.C. Tangeman, M.E. Tisack, J. Power Sources 131 (2004) 41–48.
[6] M. Schulze, T. Knori, A. Schneider, E. Gulzowa, J. Power Sources 127 (2004) 222–229.
[7] L.M. Roen, C.H. Paikz, T.D. Jarvic, Electrochem. Solid-State Lett. 7 (2004) A19–A22.
[8] W. Schmittinger, A. Vahidi, J. Power Sources 180 (2008) 1–14.
[9] K. Jayakumar, S. Pandiyan, N. Rajalakshmi, K.S. Dhathathreyan, J. Power Sources 161 (2006) 454–459.
[10] J. Yu, T. Matsuura, Y. Yoshikawa, M.N. Islam, M. Hori, Phys. Chem. Chem. Phys. 7 (2005) 373–378.
[11] B. Wahdamea, D. Candusso, F. Harel, X. François, M.-C. Pera, D. Hissel, J.-M. Kauffmann, J. Power Sources 182 (2008) 429–440.
[12] S. Yoshioka, A. Yoshimura, H. Fukumoto, O. Hiroi, H. Yoshiyasu, J. Power Sources 144 (2005) 146–151.
[13] Z. Qi, A. Kaufman, J. Power Sources 109 (2002) 469–476.
[14] M. Millera, A. Bazylaka, J. Power Sources 196 (2011) 601–613.
[15] C. Sishtla, G. Koncar, R. Platon, S. Gamburzev, A.J. Appleby, O.A. Velev, J. Power Sources 71 (1998) 249–255.
[16] K.-S. Lee, B.-S. Lee, S.J. Yoo, S.-K. Kim, S.J. Hwang, H.-J. Kim, E. Cho, D. Henkensmeier, J.W. Yun, S.W. Nam, T.-H. Lim, J.H. Jang, Int. J. Hydrogen Energy 37 (2012) 5891–5900.
[17] Z. Luo, D. Li, H. Tang, M. Pan, R. Ruan, Int. J. Hydrogen Energy 31 (2006) 1831–1837.
[18] S.-Y. Ahn, S.-J. Shin, H.Y. Ha, S.-A. Hong, Y.-C. Lee, T.W. Lim, I.-H. Oh, J. Power Sources 106 (2002) 295–303.
[19] G. Lee, M. Jung, S. Ryoo, M. Park, S. Ha, S. Kim, Int. J. Hydrogen Energy 35 (2010) 13131–13136.
[20] J. Scholta, N. Berg, P. Wilde, L. Jörissen, J. Garche, J. Power Sources 127 (2004) 206–212.
[21] E.A. Cho, U.-S. Jeon, S.-A. Hong, I.-H. Oh, S.-G. Kang, J. Power Sources 142 (2005) 177–183.
[22] H. Tawfik, Y. Hung, D. Mahajan, J. Power Sources 163 (2007) 755–767.
[23] R.A. Antunes, M.C.L. Oliveira, G. Ett, V. Ett, Int. J. Hydrogen Energy 35 (2010) 3632–3647.
[24] J. André, L. Antoni, J.-P. Petit, Int. J. Hydrogen Energy 35 (2010) 3684–3697.
[25] S. Ahn, S. Shin, H. Ha, S. Hong, Y. Lee, T. Lim, I.-H. Oh, J. Power Sources 106 (2002) 295–303.
[26] X. Yuan, S. Zhang, H. Wang, J. Wu, J.C. Sun, R. Hiesgen, K.A. Friedrich, M. Schulze, A. Haug, J. Power Sources 195 (2010) 7594–7599.
[27] J. Li, K. Wang, Y. Yang, ECS Trans. 25 (2009) 385–394.
[28] W. Mérida, D.A. Harrington, J.M. Le Canut, G. McLean, J. Power Sources 161 (2006) 264–274.
[29] J. Kim, I. Lee, Y. Tak, B.H. Cho, Renew. Energy 51 (2013) 302–309.
[30] D.G. Sanchez, P.L. Garcia-Ybarra, Int. J. Hydrogen Energy 37 (2012) 7279–7288.
[31] K.D. Baik, I.M. Kong, B.K. Hong, S.H. Kim, M.S. Kim, Appl. Energy 101 (2013) 560–566.
[32] M. Inaba, T. Kinumoto, M. Kiriake, R. Umebayashi, A. Tasaka, Z. Ogumi, Electrochim. Acta 51 (2006) 5746–5753.
[33] T.E. Springer, T.A. Zawodzinski, M.S. Wilson, S. Gottesfeld, J. Electrochem. Soc. 143 (1996) 587–599.
[34] T.J.P. Freire, E.R. Gonzalez, J. Electroanal. Chem. 503 (2001) 57–68.
[35] V.A. Paganin, C.L.F. Oliveira, E.A. Ticianelli, T.E. Springer, E.R. Gonzalez, Electrochim. Acta 43 (1998) 3761–3766.
[36] H.-T. Kim, K.-Y. Song, T.V. Reshetenko, S.-I. Han, T.-Y. Kim, S.-Y. Cho, M.-K. Min, G.-S. Chai, S.-C. Shin, J. Power Sources 193 (2009) 515–522.
[37] Y. Yu, H. Li, H. Wang, X.-Z. Yuan, G. Wang, M. Pan, J. Power Sources 205 (2012) 10–23.
[38] S.J. Bae, S.-J. Kim, J. In Park, C.W. Park, J.-H. Lee, I. Song, N. Lee, K.-B. Kim, J.-Y. Park, 37 (2012) 9775–9781.
[39] Y. Yu, X.-Z. Yuan, H. Li, E. Gu, H. Wang, G. Wang, M. Pan, Int. J. Hydrogen Energy 37 (2012) 15288–15300.
[40] D. Zhao, B.L. Yi, H.M. Zhang, H.M. Yu, L. Wang, Y.W. Ma, D.M. Xing, J. Power Sources 190 (2009) 301–306.
[41] J. Xie, D.L. Wood, D.M. Wayne, T.A. Zawodzinski, P. Atanassov, R.L. Borup, J. Electrochem. Soc. 152 (2005) A104–A113.
[42] L. Merlo, A. Ghielmi, L. Cirillo, M. Gebert, V. Arcella, J. Power Sources 171 (2007) 140–147.